Intramolecular Electron Transfer in Lysozyme Studied by Time-Resolved Chemically Induced Dynamic Nuclear Polarization

Olga B. Morozova,[†] P. J. Hore,[‡] Renad Z. Sagdeev,[†,§] and Alexandra V. Yurkovskaya*[,†]

International Tomography Center of SB RAS, 630090, Institutskaya 3a, Novosibirsk, Russia, Department of Chemistry, Oxford University, Physical and Theoretical Chemistry Laboratory, Oxford University, South Parks Road, Oxford, OX1 3QZ, United Kingdom, and Center of Magnetic Tomography and Spectroscopy, Moscow State University, 119992, Leninskie Gory 1-73, Moscow, Russia

Received: June 22, 2005; In Final Form: September 2, 2005

The kinetics of the chemically induced dynamic nuclear polarization (CIDNP) produced in reactions of hen lysozyme with photosensitizers have been studied for the native state of the protein at pH 3.8 and for two denatured states. The latter were generated by raising the temperature to 80 °C or by combining a temperature rise (to 50 °C) with the addition of chemical denaturant (10 M urea). Detailed analysis of the CIDNP time dependence on a microsecond time scale revealed that, in both denatured states, intramolecular electron transfer (IET) from a tyrosine residue to the cation radical of a tryptophan residue (rate constant k_f) is highly efficient and plays a decisive role in the evolution of the nuclear polarization. To describe the observed CIDNP kinetics with a self-consistent set of parameters, IET in the reverse direction, from a tryptophan residue to a tyrosine residue radical (rate constant k_r), has also to be taken into account. The IET rate constants determined by analysis of the CIDNP kinetics are, at 80 °C: $k_f = 1 \times 10^5\ s^{-1}$ and $k_r = 1 \times 10^4\ s^{-1}$; at 50 °C in the presence of 10 M urea: $k_f = 7 \times 10^4\ s^{-1}$, $k_r = 1 \times 10^4\ s^{-1}$. IET does not appear to influence the CIDNP kinetics of the native state.

Introduction

Studies of the functions of proteins within cells and in vitro systems have shown that unfolded states of proteins have an important role to play in numerous cellular processes and signaling events (see ref 1 and references therein). In contrast to techniques that use optical spectroscopy to monitor protein folding, nuclear magnetic resonance (NMR) spectroscopy is capable of probing events at the level of individual amino acid residues but suffers from rather low sensitivity.[2] A partial solution to this problem lies in a related technique based on the phenomenon of chemically induced dynamic nuclear polarization (CIDNP) in which the intensities of certain NMR lines in the spectrum of a protein are selectively enhanced.[3−7] By addition to a solution of the protein a small quantity of a photosensitizer, usually a flavin, and irradiation of the sample inside the NMR probe with a laser, nuclear polarization can be generated in the side chains of histidine (His), tryptophan (Trp), and tyrosine (Tyr) residues provided they are physically accessible to, and therefore reactive with, the photosensitizer. The signal enhancements obtained from these cyclic photochemical reactions, which produce no net chemical change in the protein, have been used to study the surface structures of proteins and protein−ligand interactions and have recently been employed to follow protein folding reactions in real time, at the level of individual amino acid residues, with about 100 ms time resolution.[5,8−10] In addition to the remarkable sensitivity enhancement, CIDNP contains information on transient reaction intermediates and on free radical reaction pathways encoded in the strongly perturbed NMR intensities of the stable diamagnetic reaction products.

Hen egg white lysozyme has been extensively used in the development of protein NMR techniques, not only for studying native[11] and unfolded[8,12,13] proteins in solution but also as a test case in a real-time CIDNP study of kinetic intermediates in protein folding reactions.[9,14] Signal intensities detected for tryptophan and tyrosine residues in such experiments were interpreted in terms of the changes in side-chain accessibility during the folding process. Under the steady-state conditions of these measurements (with time resolution of ∼100 ms), the observed CIDNP intensities can be complicated by the creation of nuclear polarization in random radical encounters in solution and by nuclear paramagnetic relaxation in the radicals and are not necessarily directly related to the accessibility of the exposed aromatic amino acid residues on the surface of the protein molecule. An alternative approach is time-resolved (TR) CIDNP, which combines nanosecond-pulsed laser excitation with pulsed NMR detection of nuclear polarization on a microsecond time scale.[15−19] The advantage of the TR CIDNP method over its stationary analogue is the possibility of separating the geminate (nanosecond time scale) and the homogeneous (microsecond time scale) stages of the radical reactions, so allowing a quantitative kinetic analysis of the nuclear polarization.

To interpret changes in CIDNP intensities in the course of a protein folding reaction, one needs an understanding of the formation of nuclear polarization in the denatured and native states that constitute the initial and final states of the folding process. Lysozyme was the subject of our first comparative TR CIDNP study of proteins in native and denatured states.[17] A significant difference was detected between the CIDNP kinetics of the native state, at pH 3.8, and the denatured states obtained in the presence of 10 M urea at 50 °C and at temperatures above

* To whom correspondence should be addressed. Phone: +7(3832)-331333. Fax: +7(3832)331399. E-mail: yurk@tomo.nsc.ru.
[†] International Tomography Center of SB RAS.
[‡] Oxford University.
[§] Moscow State University.

10.1021/jp053394v CCC: $30.25
Published on Web 11/01/2005

70 °C in the absence of chemical denaturant.[17] While the CIDNP intensities of the native state showed only a slight time dependence between 1 μs and 1 ms, a significant growth in the tyrosine signal and a fast decay of the tryptophan signal were observed for both denatured states. On the basis of the close similarity of the CIDNP kinetics of the denatured protein and of the tryptophan−tyrosine dipeptide (Trp−Tyr),[17,20−22] we tentatively attributed the observed time dependence to the influence of intramolecular electron transfer (IET) from tyrosine residues to the cation radicals derived from tryptophan residues in the denatured states of the protein.[17] Our recent detailed investigation of CIDNP in Trp−Tyr has shown that the reactivity of the amino acids toward photoexcited dyes changes when they are linked into peptides, that the efficiency of IET depends on pH, and that IET is reversible under acidic conditions.[20]

Armed with this knowledge, in the present paper we apply the kinetic scheme developed to describe the behavior of Trp−Tyr as part of a detailed investigation of CIDNP kinetics in the native and denatured states of lysozyme. Model simulations have given a consistent set of kinetic parameters to describe the dynamic processes of intramolecular electron migration in unfolded proteins and in particular have demonstrated the high efficiency and slight reversibility of IET in the denatured protein. The correlation times of the intramolecular motions of the spin-polarized residues in lysozyme have been estimated from the paramagnetic nuclear spin−lattice relaxation times, T_1, in the radicals. These results give a clearer picture of the origin of the differences between the CIDNP behavior of native and denatured states of lysozyme.[9,13,14]

Experimental

A detailed description of the TR CIDNP apparatus has been given earlier.[18] The samples, sealed in a standard 5-mm NMR Pyrex ampule, were irradiated by a COMPEX Lambda Physik excimer laser (wavelength 308 nm, pulse energy up to 150 mJ) in the probe of a 200-MHz Bruker DPX-200 NMR spectrometer. Light was guided to the sample using an optical system comprising a quartz lens, a prism, and a cylindrical light guide (8 mm diameter). TR CIDNP experiments were carried out with the pulse sequence: radio frequency (RF) saturation pulses, laser pulse, evolution time τ, RF detection pulse, free induction decay. As the background signals in the spectrum originating from equilibrium polarization are suppressed, only resonances from the polarized products formed during the variable delay τ appear in the CIDNP spectra. In all kinetic measurements, a RF pulse with duration 4 μs was used. The timing corresponds to the center of the RF pulse (e.g., $\tau = 2$ μs for an RF pulse immediately following the laser flash) on all plots in Figures 3 and 5.

Hen lysozyme, 2,2′-dipyridyl (DP), flavin mononucleotide (FMN), urea-d_4, DCl, and D_2O were used as received from Sigma-Aldrich. The sample concentrations were: 0.7 mM protein, 0.5 mM DP, and 1.6 mM FMN. The pH was adjusted by addition of small quantities of DCl. No correction for the deuterium isotope effect on the pH was made.

Results

The structure of lysozyme consists of two domains separated by the active site: (1) the α-domain (residues 1−35 and 85−129), which includes four helices, two at the C-terminus and two at the N-terminus, and a short 3_{10}-helix; (2) the β-domain (residues 36−84) which contains a triple-stranded antiparallel β-sheet, another 3_{10}-helix, and a large loop region. Figure 1 shows a representation of the solution state NMR structure of

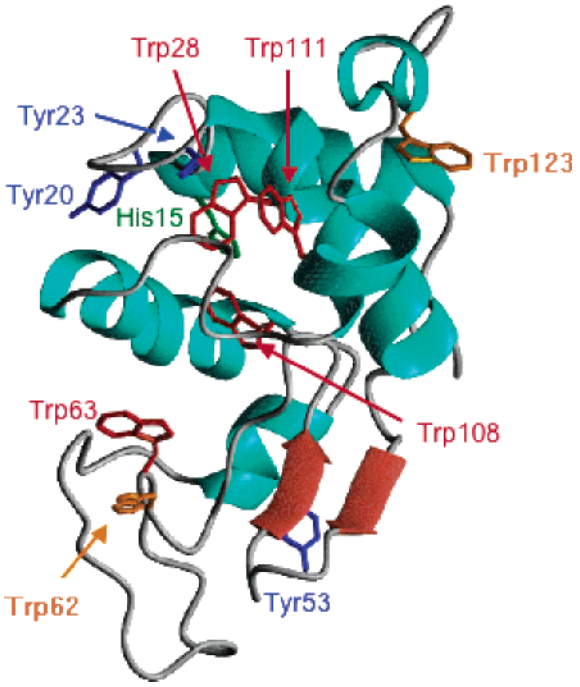

Figure 1. The structure of hen lysozyme (PDB file 1E8L[23]). The most solvent-accessible tryptophan residues (62 and 123) are shown in orange; the other tryptophan residues are in red. Tyrosine and histidine residues are shown in blue and green, respectively. The figure was drawn using MOLMOL.[25]

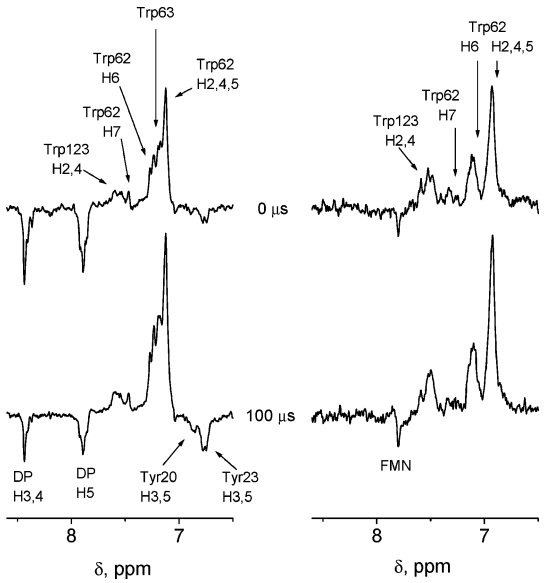

Figure 2. Aromatic region of the ^{1}H CIDNP spectra obtained for native lysozyme with DP (left) and FMN (right) at pH 3.8. The upper spectra were taken immediately after the laser pulse and the lower spectra at 100 μs.

lysozyme, refined using residual dipolar coupling data.[23] The potentially CIDNP-active residues are Tyr20, 23, and 53, Trp28, 62, 63, 108, 111, and 123, and His15.

Figure 2 shows ^{1}H CIDNP spectra of native lysozyme with DP (left) and FMN (right) as the sensitizer. The upper pair of spectra were recorded immediately after the laser pulse ($\tau = 0$) and the lower pair at $\tau = 100$ μs. The spectrum generated using FMN is very similar to that recorded earlier using the steady-state CIDNP method:[11,14] enhancements are observed for the protons of the most exposed residues, Trp62 and Trp123. With DP as the photosensitizer, the spectra are somewhat different. Additional resonances appear between those of H6 and H2,4

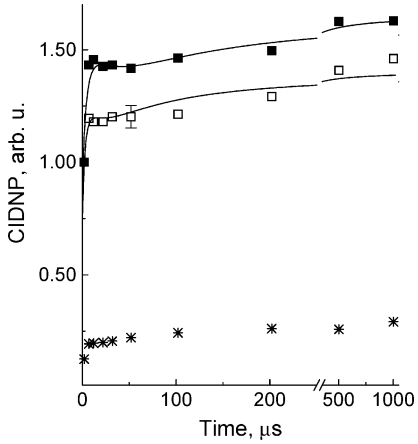

Figure 3. [1]H CIDNP kinetics, obtained for different protons of native lysozyme at pH 3.8: H2,6 of Trp62 and Trp63 with DP (solid squares); H2,6 of Trp62 with FMN (open squares); H3,5 of Tyr20 with DP (stars). The lines are simulations (see text) using the parameter values listed in Table 1.

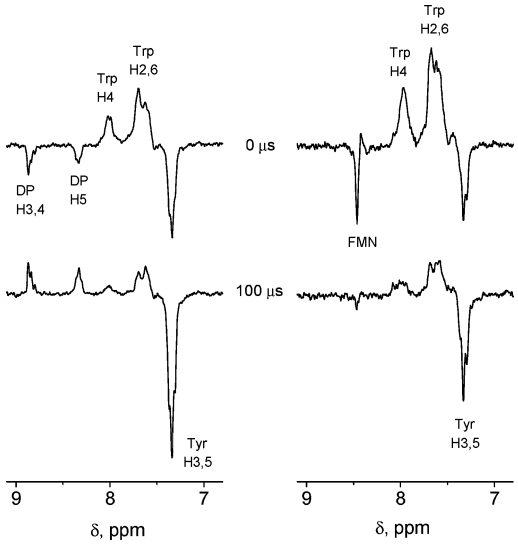

Figure 4. Aromatic region of [1]H CIDNP spectra obtained for denatured lysozyme with DP (left) and FMN (right) at pH 3.8 and 80 °C. The upper spectra were taken immediately after the laser pulse, and the lower spectra at 100 μs.

of Trp62 as indicated in Figure 2, and two weak emissive signals are observed at 6.89 and 6.76 ppm, close to the chemical shifts reported for H3,5 of Tyr20 and Tyr23.[24] A weak CIDNP signal from Tyr23 has been observed earlier.[11] The enhanced absorption between the resonances of H6 and H2,4 of Trp62 decreases noticeably in the presence of *N*-acetylglucosamine (not shown), an inhibitor that binds in the active site cleft close to Trp62 and Trp63. Thus, we attribute this additional signal to Trp63. Although the CIDNP pattern obtained with FMN is similar to that reported earlier using 3-*N*-carboxymethyl-lumiflavin,[11] the resonances of Trp62 are shifted by 0.2 ppm toward high field which may indicate weak protein−flavin binding.

The CIDNP kinetics for the protons of native lysozyme are shown in Figure 3. The experimental points obtained with DP (solid squares) correspond to the sum of the intensities for the two residues, Trp62 and Trp63, since they could not be separated in the spectrum (integration limits from 7.05 to 7.35 ppm). The experimental points obtained with FMN (open squares) refer to the signals of Trp62 only (integration limits from 6.75 to 7.20 ppm). The intensities of the Trp signals with both sensitizers were taken as equal to unity at $\tau = 0$. The tyrosine

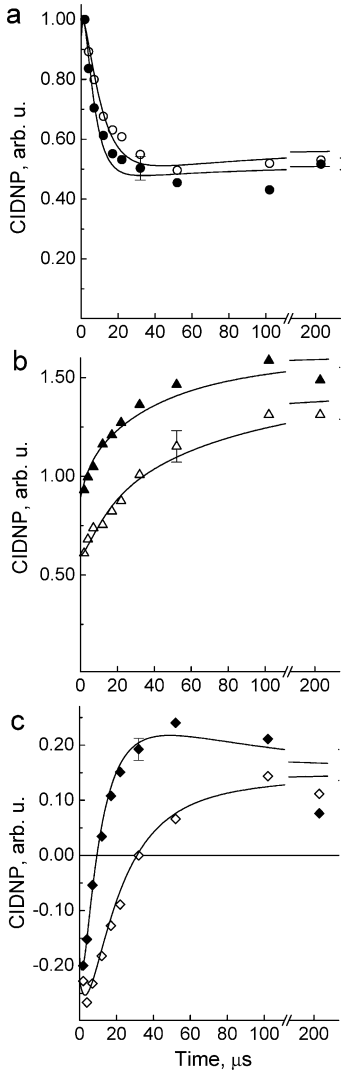

Figure 5. [1]H CIDNP kinetics, obtained for denatured lysozyme with DP: H2,6 of Trp (squares), H3,5 of Tyr (triangles), H3,4 of DP (diamonds). Solid symbols: 80 °C; open symbols: 50 °C, 10 M urea-d_4. The lines are simulations (see text) using the parameter values listed in Table 1.

signals were scaled in accord with the relative intensities of peaks in the spectra obtained with DP. Both sets of Trp kinetics are characterized by a maximum at around 10 μs that is more pronounced for DP and a small monotonic growth after 50 μs. The nuclear polarization of the H3,5 protons of tyrosine increases slightly with increasing τ (Figure 3, stars).

Denatured lysozyme was obtained under the following experimental conditions: (a) 80 °C at pH 3.8, and (b) 50 °C in the presence of 10 M urea-d_4, also at pH 3.8. Figure 4 shows CIDNP spectra of thermally denatured lysozyme, polarized by reaction with DP (left) and FMN (right), recorded immediately after the laser pulse (upper spectra) and at $\tau = 100$ μs (lower spectra). In contrast to the native protein, the spectra of these denatured states are significantly time dependent. The tryptophan signals decay and the tyrosine signals grow between 0 and 100 μs, whichever sensitizer is used. The most pronounced changes are observed for the resonances of DP, for which the polarization changes from emission to enhanced absorption. Qualitatively the same behavior was found at 50 °C in the presence of 10 M urea-d_4 (not shown).

The CIDNP kinetics obtained for lysozyme with DP at 80 °C (solid symbols) and at 50 °C in the presence of 10 M urea (open symbols) are shown in parts a−c of Figure 5. The

CIDNP intensity of the Trp H2,6 resonance at $\tau = 0$ is taken as unity in each case, and the signals of Tyr and DP are rescaled accordingly. The evolution of the nuclear polarization is slower in the presence of urea, an effect that is most pronounced for the DP protons.

Discussion

CIDNP Spectra of the Native State. CIDNP-active amino acid residues competing for reaction with photoexcited triplet dye molecules are characterized by quenching rate constants that can be treated as a product of the quenching rate constant of a fully accessible residue and a factor reflecting the accessibility of the residue. At pH 3.8, the mechanism of quenching of the triplet states of FMN and of DP, by tryptophan or tyrosine is electron transfer with rate constants of the order of 10^9 M^{-1} s^{-1}.[26−28]

By use of the PDB file 1E8L[23] and a probe size of 1.4 Å, we calculated the following total side-chain accessibilities (TSA) of the polarized residues of lysozyme as the percentage of accessible surface area for the entire side chain of the residue relative to the surface accessibility of the same residue type in an Ala-X-Ala tripeptide):[29] 68.5% (Trp62), 15.2% (Trp63), 15.7% (Trp123), 31.2% (Tyr20), and 17.3% (Tyr23). It can be seen from Figure 2 that the signal intensities in the spectra recorded at $\tau = 0$ do not fully correlate with the TSAs. Tyr20, which has the highest accessibility after Trp62, is only slightly polarized by DP and does not appear in the spectra generated with FMN. Trp123 and Trp63 have comparable accessibilities and similar CIDNP intensities with DP, whereas in the spectrum with FMN, no signal from Trp63 is observed. This difference in the CIDNP patterns can be attributed to the difference in hydrodynamic radii of the two dyes. From NMR diffusion measurements, radii of 3 Å for DP and 5 Å for FMN were obtained. The larger size of FMN presumably restricts its penetration into the active cite cleft where Trp63 is located. Thus, side-chain accessibility in the context of CIDNP is a combined property of the residue and the dye. Such a threshold effect was also observed for Tyr103 in bovine α-lactalbumin, which is polarizable by DP but not FMN.[18]

CIDNP Kinetics. In an earlier publication, we interpreted the CIDNP kinetics of denatured lysozyme in terms of the important role played by IET from a tyrosine residue to the cation radical of a tryptophan residue.[17] IET has been extensively studied using pulse radiolysis in a number of peptides containing tryptophan and tyrosine[30−34] as well as in lysozyme.[35,36] Its influence on CIDNP has been examined for the dipeptide Trp−Tyr:[20−22] the rate constant strongly depends on the protonation state of the tryptophan radical,[22] which can exist in cationic or neutral forms ($pK_a = 4.3$ for free tryptophan,[37] and $4.6 < pK_a < 5.4$ for tryptophan in peptides[38,39]). It has also been established that a decrease in pH accelerates IET in the reverse direction, i.e., from tryptophan residues to tyrosine radicals.[20] The relevant reactions are given in eq 5 below, in which TrpH and TyrOH are the amino acid residues in the peptide or protein. For Trp−Tyr, $k_f = 5.5 \times 10^5$ s^{-1} in D_2O at room temperature, and $\log(K) = \log(k_f/k_r)$ was found to depend linearly on pH with a slope equal to unity.[20] The condition $K = 1$ is met at pH 1.4. At pH 3.8, at room temperature, k_r is smaller than k_f by more than an order of magnitude, and electron transfer can be treated as irreversible.[20,21] The strong attenuation in the CIDNP signal intensity at higher temperatures made it impossible to measure the CIDNP kinetics of Trp−Tyr under the denaturing conditions used in the present work. It can be anticipated that a rise in temperature will increase both k_f and k_r.

In a solution containing 10 M urea-d_4, $\log(K)$ was also found to be a linear function of pH but with a slope equal to 0.4; furthermore, $K = 1$ at pH 1.6.[20] This means that, at a given pH, the IET reaction has a higher reversibility in the presence of urea. The rate constant, k_f, is reduced by the presence of 10 M urea (to 3.0×10^5 s^{-1})[20] and an estimate, based on data in ref 20, gives $K \approx 6$ at pH 3.8.

The kinetics of the nuclear polarization observed for denatured lysozyme closely resemble those of Trp−Tyr under acidic conditions at pH > 2.4:[20−22] the decay of the Trp signals, the growth of the Tyr intensities, and the change of sign from emission to enhanced absorption for DP are characteristic of a dominant electron transfer from tyrosine residues to oxidized tryptophan residues. To interpret the CIDNP kinetics for lysozyme, we have consequently adopted the reaction scheme used successfully to account for the behavior of Trp−Tyr, with bidirectional IET. The reaction steps are as follows (where TrpH and TyrOH are the amino acid residues in the peptide or protein)

$$DPH^+ \xrightarrow{h\nu} {}^SDPH^+ \rightarrow {}^TDPH^+ \quad (1)$$

$${}^TDPH^+ + TrpH{-}TyrOH \rightarrow DPH^\bullet + TrpH^{\bullet+}{-}TyrOH,\ [\alpha R_0] \quad (2)$$

$${}^TDPH^+ + TrpH{-}TyrOH \rightarrow DPH^\bullet + H^+ + TrpH{-}TyrO^\bullet,\ [(1-\alpha)R_0] \quad (3)$$

$$DPH^\bullet + H^+ \rightarrow DPH_2^{\bullet+},\ [R_0] \quad (4)$$

$$TrpH^{\bullet+}{-}TyrOH \underset{k_r}{\overset{k_f}{\rightleftharpoons}} TrpH{-}TyrO^\bullet + H^+ \quad (5)$$

$$DPH_2^{\bullet+} + TrpH^{\bullet+}{-}TyrOH \xrightarrow{k_1} DPH^+ + TrpH{-}TyrOH + H^+ \quad (6)$$

$$DPH_2^{\bullet+} + TrpH{-}TyrO^\bullet \xrightarrow{k_2} DPH^+ + TrpH{-}TyrOH \quad (7)$$

$$TrpH^{\bullet+}{-}TyrOH + TrpH{-}TyrOH \xrightarrow{k_{ex}} TrpH{-}TyrOH + TrpH^{\bullet+}{-}TyrOH \quad (8)$$

Steps 1−4 represent light absorption and intersystem crossing to form the protonated triplet state of DP, reaction by intermolecular electron transfer to form radicals from either a tryptophan residue or a tyrosine residue, and subsequent protonation of the neutral DP radical. All four processes are too fast to be resolved in the present experiments and are treated as occurring instantaneously; their net result is geminate nuclear polarization that is effectively present immediately after the laser pulse. As indicated, the initial concentrations of radicals are: αR_0 ($TrpH^{\bullet+}$), $(1-\alpha)R_0$ ($TyrO^\bullet$), and R_0 ($DPH_2^{\bullet+}$). Step 5 is the reversible IET described above. Steps 6 and 7 are second-order radical recombination reactions, and step 8 is the degenerate electron exchange of the $TrpH^{\bullet+}$ radicals (a process that is negligibly slow for $TyrO^\bullet$ radicals at the pH values studied here). These last three reactions can influence the observed CIDNP kinetics because they transfer polarization from radicals to ground state molecules. Nuclear polarization from the radicals that survive the geminate recombination reaction is superimposed on the geminate polarization of opposite phase, so canceling part of the observable polarization. Cancellation is

TABLE 1: Parameters Obtained from Simulation of ^{1}H CIDNP Kinetics of Hen Lysozyme: Second Order Termination Parameters, Nuclear Paramagnetic Relaxation Times, and Rate Constants of Intramolecular Electron Transfer

state	sensitizer	R_0k_t/s^{-1}	$T_1/\mu s$ (Trp)	$T_1/\mu s$ (Tyr)	k_f/s^{-1}	k_r/s^{-1}	k_{ex}/s^{-1}
native	DP	8.5×10^4	43	n/d[a]	$<5 \times 10^3$	$<5 \times 10^3$	$<5 \times 10^3$
	FMN	1.3×10^5	27	n/d[b]	$<5 \times 10^3$	$<5 \times 10^3$	$<5 \times 10^3$
temperature denatured	DP	1.5×10^5	18	16	1×10^5	1×10^4	5×10^5
urea denatured	DP	5.5×10^4	27	31	7×10^4	1×10^4	3.5×10^5

[a] T_1 for Tyr was not determined because the signal/noise ratio was too low for quantitative evaluation of the data. [b] Tyr is not polarized with FMN.

usually incomplete due to loss of polarization by nuclear spin−lattice relaxation in the radicals (with relaxation times $T_{1,Trp}$ and $T_{1,Tyr}$).

Furthermore, when independently formed radicals from the amino acid residue and the dye encounter to form a radical pair, additional "F-pair" polarization is created, the sign of which is the same as that arising from a geminate radical pair with a triplet precursor. This mechanism is responsible for the formation of CIDNP in the reactions of tyrosine radicals created by IET, since these radicals have no geminate nuclear polarization.

The decay of the Trp polarization and the growth of the Tyr polarization does not provide conclusive evidence for the existence of IET. Fast decay may be the result of degenerate electron exchange, and growing CIDNP signals could be obtained for certain combinations of the second-order termination rate constant, initial radical concentration, and the nuclear paramagnetic relaxation time, without taking IET into account. More convincing evidence for the importance of IET is the inversion of the phase of the polarization observed for the DP protons. The *g*-values of the participating radicals increase in the sequence g(Trp) < g(DP) < g(Tyr), so that the sign of the DP polarization depends on the identity of the partner radical. An initially emissive enhancement for DP reflects a predominance of radical pairs containing a Trp radical, formed from triplet DP by electron transfer. IET increases the yield of Tyr radicals, such that the polarization may change its sign at later times. In no other way can DP acquire positive polarization comparable in magnitude to the negative polarization present immediately after the laser flash (as observed in Figure 5c).

With FMN as the photosensitizer, the Trp and Tyr residues in lysozyme demonstrate qualitatively similar CIDNP kinetic behavior. The sign of the polarization of the FMN protons does not change as τ is increased, since in the 4.7-T magnetic field of the NMR spectrometer, the CIDNP enhancements are much larger in the flavin/tryptophan radical pair than they are in the flavin/tyrosine radical pair, making the CIDNP kinetics of FMN less sensitive to IET. Thus, for quantitative analysis, we have chosen to focus on the kinetics obtained with DP, noting that the rate of IET is independent of the sensitizer.

To simulate the CIDNP kinetics in Trp−Tyr, we adopted the general approach suggested by Fischer[40] as used previously for the reversible radical photoreactions of DP with individual amino acids.[26,27,41] Full details are given in ref 20. The same approach was used to interpret the observations reported above for denatured lysozyme with some minor differences mentioned below. Strictly speaking, different values of k_f and k_r should be associated with each pair of Trp/Tyr residues undergoing IET. However, since the contributions from individual pairs of residues could not be separated in the spectra, we use a single pair of rate constants corresponding to a weighted average over all contributing pairs of Trp/Tyr residues, which may include those that are not accessible in the native state. Since lysozyme contains six tryptophan residues, degenerate exchange is treated as an irreversible intramolecular process.

To reduce the number of fitting parameters, we fixed the ratio of the nuclear polarizations of DP in the radical pairs with Trp and Tyr counter-radicals at 1.1, as found for Trp−Tyr and for a mixture of the amino acids,[21] and the two recombination rate constants were assumed to be identical ($k_1 = k_2 = k_t$). The ratio of the polarizations created in geminate and F pairs, γ, was taken as 2.8, as suggested by Fischer,[40] except for the tyrosine residues, for which $\gamma = 1.4$ in acidic solution.[27] The fitting parameters were: R_0k_t, k_f, k_r, k_{ex}, $T_{1,Trp}$, and $T_{1,Tyr}$ and the scaling factors associated with the geminate polarizations. The kinetics of DP and Tyr are highly sensitive to the parameter α, which was calculated from the ratio of corresponding quenching rate constants for Trp−Tyr at 80 °C and 50 °C, 10 M urea. Values of the proton T_1 of $DPH_2^{\bullet+}$ were calculated using the temperature dependence of the rotational correlation time and the value of T_1 at room temperature (100 μs), as follows: 370 μs at 80 °C and 120 μs at 50 °C, 10 M urea. Data for dipyridyl (Figure 5c) obtained for times longer than 200 μs (not shown) show deviations from the simulated kinetics: the CIDNP amplitude slowly decreases to zero as τ is increased to 1 ms. We believe that, under our experimental conditions, radical processes are over by 200 μs, on the basis that the CIDNP amplitudes of Trp and Tyr have reached stationary values by this time, indicating that the concentration of radicals has reached a negligible level. At present, we have no definitive explanation for the decay of the DP polarization. Although it would have been possible to expand the parameter space to include a further rate constant to account for the slow decay of the DP signal, it seemed more sensible to focus on the inherently more interesting paramagnetic stage of the reaction for $\tau < 100$ μs.

The best-fit parameters are listed in Table 1 for simultaneous fits to the three sets of data, for Trp and Tyr residues, and for DP. The confidence intervals for the best-fit parameters are estimated at 20% of the parameter values. For tryptophan, the rapid decay of the CIDNP kinetics could not be reproduced with the values of k_f needed to fit the kinetics of DP and Tyr: as a result it was necessary to take into account degenerate electron exchange between Trp residues as indicated in eq 8. To determine whether this process is inter- or intramolecular, we also measured the CIDNP kinetics at a protein concentration of 0.35 mM at 80 °C (not shown). The kinetics under these conditions were simulated using the same parameter values except for a smaller value of R_0k_t. So we conclude that the degenerate electron exchange is an intramolecular process involving pairs of tryptophan residues within a single protein molecule and that the deceleration of the bimolecular termination rate originates from the smaller concentration of radical pairs formed by triplet quenching at the lower protein concentration.

It is fortunate that the characteristic times of the IET processes in denatured lysozyme fall within the "kinetic window" of time-resolved CIDNP, which ranges from ~100 ns to ~100 μs, making it possible to determine both forward and backward rate constants. The efficiency of IET between oxidized Trp and Tyr residues decreases with the distance between the two species.

It would be improper to compare directly the value of k_f obtained in the present study for denatured protein with the corresponding rate constant for the Trp−Tyr dipeptide (5.5×10^5 s^{-1}) at ambient temperature, because the rate constants inevitably increase with temperature. Nevertheless, our values of k_f and k_r are lower than those for the dipeptide, consistent with the separation in the peptide being shorter than the average distance between interacting Tyr−Trp pairs in the denatured protein.

Although the reversibility of reaction 5 as determined from the CIDNP kinetics is not very high ($K = 10$ at 80 °C and $K = 7$ at 50 °C, 10 M urea), its inclusion improved the optimum fit for tyrosine (the sum of squared residuals was reduced by a factor of 2). Also, without taking into account the reversibility of IET, attempts to fit the Trp kinetics at 50 °C and 10 M urea required a rate constant for degenerate electron exchange, $k_{ex} = 8 \times 10^5$ s^{-1}, which is higher than the value required at 80 °C ($k_{ex} = 5 \times 10^5$ s^{-1}), contrary to the expectation that k_{ex} should increase with temperature.

The difference in second-order termination rates in the two types of denaturing conditions reflects the different viscosities in the two cases. Extrapolation of the viscosity of aqueous urea solutions to a concentration of 10 M at room temperature gives a 2-fold increase in viscosity relative to pure water. If we assume the same dependence at 50 °C, then the estimated viscosity of 10 M urea in water at 50 °C is about three times higher than that of water at 80 °C. This agrees well with the 2.5-fold difference in termination rates obtained from the CIDNP kinetics.

At 50 °C and 10 M urea, the stationary polarization of tyrosine (i.e., at $\tau = 200$ μs) exceeds the geminate polarization by more than a factor of 2, whereas at 80 °C this ratio is smaller, about 1.6, though the latter corresponds to a higher value of k_f. Two factors govern the increase in the Tyr CIDNP as a function of time. First, for smaller values of R_0k_t, the radicals live longer and spin−lattice relaxation removes the escape polarization more efficiently, leading to more effective formation of F-pair polarization. Second, when more Trp radicals are initially formed relative to Tyr radicals, a larger number of them can be converted into Tyr radicals; in the limiting case when there are initially no Tyr radicals, the Tyr polarization increases from zero to the stationary value formed in the F pairs. Thus, the difference in the stationary polarization values for the two sets of data for the Tyr residues in Figure 5b is less pronounced than the difference in the CIDNP detected immediately after the laser pulse.

The CIDNP kinetics of the native state of lysozyme with both dyes were simulated using a simpler procedure, without taking IET into account. The best-fit simulations (solid lines in Figure 3) were obtained using the parameter values listed in Table 1. It proved impossible to achieve satisfactory fits using a single value of $T_{1,Trp}$ for the kinetics detected with DP and with FMN. A possible reason for this discrepancy is that Trp63 has a $T_{1,Trp}$ that is different from that of Trp62 and contributes to the analyzed intensity of the Trp signal produced by DP. However, this is unlikely because the relative signal intensities do not change with time (compare the CIDNP patterns of Trp62 and Trp63 at $\tau = 0$ and at $\tau = 100$ μs in Figure 2). An alternative explanation for this discrepancy could be weak binding of FMN to lysozyme in the vicinity of the active site cleft, as evidenced by the 0.2-ppm chemical shift change for Trp62 in the presence of FMN (see above). This binding may be caused by the Coulombic interaction of the anionic phosphate group of FMN with the cationic surface of the protein, an effect that has recently been observed by transient absorption in the reaction of FMN with lysozyme.[42] A similar discrepancy in the T_1 values for tryptophan residues obtained in reactions with the two dyes has been reported for native α-lactalbumins.[18]

To check whether IET has a significant effect for the native state, we used the procedure described above for simulating the kinetics of the denatured states to fit the Trp kinetics in the native state with the two dyes. Values of k_f, k_r, and k_{ex} equal to or smaller than 5×10^3 s^{-1} had no influence on the simulated time dependence. The quality of the fit deteriorated as k_f was increased from 1×10^4 s^{-1} for zero values of k_r and k_{ex}. The values of k_f of native lysozyme in neutral solution reported earlier vary from 10^2 s^{-1},[36,43] to 10^4 s^{-1},[44] and a further increase at lower pH was reported in ref 35. No literature data for k_r and k_{ex} have been found. We also performed kinetic measurements at neutral pH: no changes in the CIDNP kinetics compared to those at pH 3.8 were observed (not shown). Thus, our data concerning the efficiency of IET in native lysozyme are in fair agreement with the data in refs 36 and 43.

Intramolecular Mobility of Residues. In aqueous solutions, ^{1}H spin relaxation in the radicals derived from small proteins operates on a microsecond time scale and is caused by fluctuation of the local magnetic fields in the radical. We use the model-free approach of Lipari and Szabo[45] for the T_1 of the protons in the radical state of the protein (pr)

$$\frac{1}{T_1(\mathrm{pr})} = (\Delta B)^2\left[\frac{S^2\tau_M}{1+[\omega_N\tau_M]^2} + \frac{(1-S^2)\tau_c(\mathrm{pr})}{1+[\omega_N\tau_c(\mathrm{pr})]^2}\right] \quad (9)$$

where ΔB is the strength of the local magnetic field whose stochastic modulation is responsible for the relaxation, ω_N is the nuclear Larmor frequency, and S^2, a generalized order parameter, is a measure of the degree of spatial restriction of the motion; the correlation time is given by $\tau_c(\mathrm{pr})^{-1} = \tau_M^{-1} + \tau_e^{-1}$, with τ_M referring to the rotation of the protein as a whole and τ_e corresponding to the intramolecular motion of the residue. For the free amino acids, assuming $S^2 = 0$ and that the rotational correlation time of the corresponding radical $\tau_c(\mathrm{aa})$ is likely to be approximately 100 ps, we have $[\omega_N\tau_c(\mathrm{aa})]^2 \ll 1$ for an NMR frequency $\omega_N = 2\pi \times 200$ MHz. Therefore

$$\frac{1}{T_1(\mathrm{aa})} = (\Delta B)^2\tau_c(\mathrm{aa}) \quad (10)$$

We further assume that ΔB is the same for the free amino acid and the corresponding residue in the protein so that we can extract information about the intramolecular mobility of the polarized residues from a comparison of the T_1 values obtained for the free amino acids and for residues in the protein. In our previous studies, we have determined the following values for the nuclear paramagnetic relaxation times, T_1(aa), in the amino acid radicals by fitting the experimental CIDNP kinetics: 63 μs for Tyr H3,5,[27] 44 μs for Trp H2,6, and 63 μs for Trp H4.[26] In the native state, the overlap of the signals of the tryptophan residues in the CIDNP spectra obtained with DP does not permit analysis of the T_1 values of individual residues, but the fact that the shape of the spectrum does not change with time allows us to conclude that the T_1 values are very similar for the three residues Trp62, Trp63, and Trp123. Values of the correlation time for the rotation of the protein molecule as a whole can be calculated from its hydrodynamic radius, R_S, using Stokes' law, $\tau_M = 4\pi\eta R_S^3/3k_BT$, in which η is the viscosity of the solution, k_B is Boltzmann's constant, and T is the temperature. Values of R_S for lysozyme in native and denatured states

were taken from ref 46. Viscosity data for aqueous solutions of urea were taken from ref 47.

Taken together, eqs 9 and 10 imply that each experimental value of $T_1(\mathrm{pr})/T_1(\mathrm{aa})$ is consistent with two values of $\tau_c(\mathrm{pr})$. For the native state, using $S^2 = 0.8$[48] and $\tau_M = 7.4$ ns, we obtained for the tryptophan residues: $\tau_c(\mathrm{pr}) = 3.7$ ns and $\tau_e = 7.8$ ns. Correlation times for the overall motion of the lysozyme molecule, τ_M, for the denatured state with urea at 50 °C and without urea at 80 °C were found to be 33 ns and 12.5 ns, respectively. There are no data reported for S^2 for the denatured states, but it is reasonable to assume that S^2 is small for both types of residues. Therefore, to calculate the correlation times for intramolecular motion, a set of three values ($S^2 = 0.0$, 0.1, and 0.2) was used. With these three values of S^2 (shown in brackets), the following values of τ_c in protein were obtained for the tryptophan residues: $\tau_c(\mathrm{pr}) = 2.3$ (0.0), 2.1 (0.1), and 1.8 (0.2) ns for the temperature-denatured state at 80 °C and 3.7 (0.0), 3.3 (0.1), and 2.9 (0.2) for the urea-denatured state at 50 °C. Each experimental value of $T_1(\mathrm{pr})/T_1(\mathrm{aa})$ corresponds to two values of $\tau_c(\mathrm{pr})$, except at the minimum of the functional dependence of the ratio $T_1(\mathrm{pr})/T_1(\mathrm{aa})$ on $\tau_c(\mathrm{pr})$, which one can obtain from eqs 9 and 10 taking the same ΔB. It is reasonable to assume that disruption of the native structure of the protein leads to a decrease in the correlation time for the internal motion of the residues. Therefore, for each value of $T_1(\mathrm{pr})/T_1(\mathrm{aa})$, we have chosen the larger $\tau_c(\mathrm{pr})$ value such that for the denatured states, $\tau_c(\mathrm{pr})$ at 80 °C is shorter than $\tau_c(\mathrm{pr})$ at 50 °C in the presence of 10 M urea-d_4.

The intramolecular correlation times, τ_e, for the tryptophan residues were determined using the corresponding $\tau_c(\mathrm{pr})$ for the three chosen values of S^2 and τ_M as follows: 4.2 (0.0), 3.7 (0.1), and 3.2 (0.2) ns for the urea-denatured state and 2.8 (0.0), 2.5 (0.1), and 2.1 (0.2) ns for the temperature-denatured state at 80 °C.

For the tyrosine residues, the signal of the native state was too weak for numerical evaluation. The correlation times $\tau_c(\mathrm{pr}) = 2.9$ (0), 2.6 (0.1), and 2.2 (0.2) ns were found for the denatured state at 50° C in the presence of 10 M urea-d_4, resulting in τ_e values of 3.2 (0), 2.8 (0.1), and 2.4 (0.2) ns. For 80 °C, it was found that a solution exists only at $S^2 = 0$, because the best fit of the CIDNP kinetics was obtained with the shortest possible T_1 assuming that ΔB in eqs 9 and 10 is the same for the amino acid and for the residue in the protein, giving $\tau_c(\mathrm{pr}) = 0.8$ ns and $\tau_e = 0.85$ ns. At all three selected values of S^2, the intramolecular correlation times τ_e for the tryptophan residues were found to be longer than those for the tyrosine residues in the temperature-denatured state at 80° C as well as for $S^2 = 0$ for the urea-denatured state at 50 °C. This finding is in agreement with the higher hydrophobicity of tryptophan residues than tyrosine residues.

Conclusion

This investigation of lysozyme in its native state and in two denatured states demonstrates that nuclear polarization is a complex function of the structural and dynamic properties of the protein. By use of the time-resolved CIDNP technique, we have shown that intramolecular electron transfer in denatured lysozyme is highly efficient and partially reversible. This reaction leads to the migration of an electron hole from tryptophan residues to tyrosine residues and affects the CIDNP kinetics such that tyrosine signals increase in time, and tryptophan signals decay rapidly. Thus, CIDNP spectra detected immediately after the laser pulse (geminate spectra) differ substantially from those detected at 200 μs, when radical reactions are complete (stationary spectra). It therefore appears that it is IET that leads to the observation of low CIDNP intensity for tryptophan residues relative to tyrosine residues in steady-state spectra rather than hydrophobic clustering as suggested earlier, although observation of IET does not exclude the existence of hydrophobic clustering. CIDNP spectra recorded immediately after a short laser pulse may thus allow a more reliable assessment of the surface accessibility of amino acid residues in proteins.

This study has shown that pulsed laser excitation with microsecond TR NMR detection can unravel complex CIDNP behavior and follow CIDNP kinetics that are determined by spin relaxation rates of nuclei in the radical intermediates and by IET reactions. By use of paramagnetic relaxation data extracted from the kinetic analysis, information can be obtained on the intramolecular mobility of residues in native and denatured states on a nanosecond time scale.

Acknowledgment. The financial support of RFBR (Project 05-03-32370), the Royal Society (International Joint Project Grant Program), and FASI (theme RI-112/001/207) is gratefully acknowledged. O.B.M. is indebted to the Russian Science Support Foundation and Young Scientists Grant Program of the President of Russian Federation (Project No. MK-2547.2005.3) for financial support. We are grateful to Dr. Ken Hun Mok for helpful discussions, measurements of hydrodynamic radii of the dyes, and for preparation of Figure 1.

References and Notes

(1) Dyson, H. J.; Wright, P. E. *Chem. Rev.* **2004**, *104*, 3607−3622.
(2) Cavanagh, J.; Fairbrother, W. J.; Palmer III, A. G.; Skelton, N. J. *Protein NMR spectroscopy: principles and practice*; Academic Press: New York, 1996.
(3) Kaptein, R. *Biol. Magn. Reson.* **1982**, *4*, 145−149.
(4) Hore, P. J.; Broadhurst, R. W. *Prog. NMR Spectroscopy* **1993**, *25*, 345−402.
(5) Mok, K. H.; Hore, P. J. *Methods* **2004**, *34*, 75−87.
(6) Kaptein, R.; Dijkstra, K.; Nicolay, K. *Nature* **1978**, *274*, 293−294.
(7) Kaptein, R. In *NMR Spectroscopy in Molecular Biology*; Pullman, B., Ed.; D. Reidel: Dordrecht, 1978; pp 211−229.
(8) Lyon, C. E.; Suh, E.-S.; Dobson, C. M.; Hore, P. J. *J. Am. Chem. Soc.* **2002**, *124*, 13018−13024.
(9) Dobson, C. M.; Hore, P. J. *Nature Struct. Biol., NMR Supp.* **1998**, *5*, 504−507.
(10) Wirmer, J.; Kuehn, T.; Schwalbe, H. *Angew. Chem.* **2001**, *113*, 4378−4380.
(11) Hore, P. J.; Kaptein, R. *Biochemistry* **1983**, *22*, 1906−1911.
(12) Mok, H. K.; Nagashima, T.; Day, I. J.; Jones, J. A.; Jones, C. J. V.; Dobson, C. M.; Hore, P. J. *J. Am. Chem. Soc.* **2003**, *125*, 12484−12492.
(13) Broadhurst, R. W.; Dobson, C. M.; Hore, P. J.; Radford, S. E.; Rees, M. L. *Biochemistry* **1991**, *30*, 405−412.
(14) Hore, P. J.; Winder, S. L.; Roberts, C. H.; Dobson, C. M. *J. Am. Chem. Soc.* **1997**, *119*, 5049−5050.
(15) Closs, G. L.; Miller, R. J. *J. Am. Chem. Soc.* **1979**, *101*, 1639−1644.
(16) Morozova, O. B.; Hore, P. J.; Bychkova, V. E.; Sagdeev, R. Z.; Yurkovskaya, A. V. *J. Phys. Chem. B* **2005**, *109*, 3668−3675.
(17) Morozova, O. B.; Yurkovskaya, A. V.; Tsentalovich, Y. P.; Forbes, M. D. E.; Hore, P. J.; Sagdeev, R. Z. *Mol. Phys.* **2002**, *100*, 1187−1195.
(18) Morozova, O. B.; Yurkovskaya, A. V.; Sagdeev, R. Z.; Mok, H. K.; Hore, P. J. *J. Phys. Chem. B* **2004**, *108*, 15355−15363.
(19) Hore, P. J.; Kaptein, R. In *NMR Spectroscopy: New Methods and Applications, ACS Symposium Series*; Levy, G. C., Ed.; American Chemical Society: Washington, 1982; pp 285−318.
(20) Morozova, O. B.; Yurkovskaya, A. V.; Sagdeev, R. Z. *J. Phys. Chem. B* **2005**, *109*, 3668−3675.
(21) Morozova, O. B.; Yurkovskaya, A. V.; Tsentalovich, Y. P.; Forbes, M. D. E.; Sagdeev, R. Z. *J. Phys. Chem. B* **2002**, *106*, 1455−1460.
(22) Morozova, O. B.; Yurkovskaya, A. V.; Vieth, H.-M.; Sagdeev, R. Z. *J. Phys. Chem. B* **2003**, *107*, 1088−1096.

(23) Schwalbe, H.; Grimshaw, S. B.; Spenser, A.; Buck, M.; Boyd, J.; Dobson, C. M.; Redfield, C.; Smith, L. J. *Protein Sci.* **2001**, *10*, 677−688.
(24) Redfield, C.; Dobson, C. M. *Biochemistry* **1988**, *27*, 122−136.
(25) Koradi, R.; Billeter, M.; Wuethrich, K. *J. Mol. Graphics* **1996**, *14*, 51−55.
(26) Tsentalovich, Y. P.; Morozova, O. B.; Yurkovskaya, A. V.; Hore, P. J. *J. Phys. Chem. A* **1999**, *103*, 5362−5368.
(27) Tsentalovich, Y. P.; Morozova, O. B. *J. Photochem. Photobiol. A: Chem.* **2000**, *30*, 33−40.
(28) Tsentalovich, Y. P.; Lopez, J. J.; Hore, P. J.; Sagdeev, R. Z. *Spectrochim. Acta, Part A* **2002**, *58*, 2043−2050.
(29) Hubbard, S. J.; Thornton, J. M. 1996, http://wolf.bi.umist.ac.uk/naccess.
(30) Faraggi, M.; DeFelippis, M. R.; Klapper, M. H. *J. Am. Chem. Soc.* **1989**, *111*, 5141−5145.
(31) Prütz, W. A.; Land, E. J.; Sloper, R. W. *J. Chem. Soc., Faraday Trans. 1* **1981**, *77*, 281−292.
(32) Mishra, A. K.; Chandrasekar, R.; Faraggi, M.; KIapper, M. H. *J. Am. Chem. Soc.* **1994**, *116*, 1414−1422.
(33) Prütz, W. A.; Siebert, F.; Butler, J.; Land, E. J.; Menez, A.; Montenay-Garestier, T. *Biochim. Biophys. Acta* **1982**, *705*, 139−149.
(34) Bobrowski, K.; Poznanski, J.; Holcman, J.; Wierzchowski, K. L. *J. Phys. Chem. B* **1999**, *103*, 10316−10324.
(35) Bobrowski, K.; Holcman, J.; Poznanski, J.; Wierzchowski, K. L. *Biophys. Chem.* **1997**, *63*, 153−166.
(36) Stuart-Audette, M.; Blouquit, Y.; Faraggi, M.; Sicard-Roselli, C.; Houee-Levin, C.; Jolle, P. *Eur. J. Biochem.* **2003**, *270*, 3565−3571.
(37) Posener, M. L.; Adams, G. E.; Wardman, P.; Cundall, R. B. *J. Chem. Soc., Faraday Trans. 1* **1976**, 2231−2239.
(38) DeFelippis, M. R.; Murthy, C. P.; Proiman, F.; Weinraub, D.; Faraggi, M.; Klapper, M. H. *J. Phys. Chem.* **1991**, *95*, 3416.
(39) Jovanovic, S. V.; Simic, M. G. *Free Radical Biol. Med.* **1985**, *1*, 125.
(40) Vollenweider, J.-K.; Fischer, H. *Chem. Phys.* **1988**, *124*, 333−345.
(41) Tsentalovich, Y. P.; Morozova, O. B.; Yurkovskaya, A. V.; Hore, P. J.; Sagdeev, R. Z. *J. Phys. Chem. A* **2000**, *104*, 6912−6916.
(42) Miura, T.; Maeda, K.; Arai, T. *J. Phys. Chem. B* **2003**, *107*, 6474−6478.
(43) Prütz, W. A.; Butler, J.; Land, E. J.; Swallow, A. J. *Biochem. Biophys. Res. Commun.* **1980**, *96*, 408−414.
(44) Bobrowski, K.; Holcman, J.; Wierzchowski, K. L. *Free Radical Res. Commun.* **1989**, *6*, 235−241.
(45) Lipari, G.; Szabo, A. *J. Am. Chem. Soc.* **1982**, *104*, 4546−4559.
(46) Wilkins, D. K.; Grimshaw, S. B.; Receveur, V.; Dobson, C. M.; Jones, J. A.; Smith, L. J. *Biochemistry* **1999**, *38*, 16424−16431.
(47) *Handbook of Chemistry and Physics*, 83rd ed.; Lide, D. R., Ed.; CRC Press: 2003.
(48) Buck, M.; Schwalbe, H.; Dobson, C. M. *J. Mol. Biol.* **1996**, *257*, 669−683.